Lawrence Berkeley National Laboratory
Recent Work

Title
Vortex Methods and Vortex Statistics

Permalink
https://escholarship.org/uc/item/49t6z1sr

Author
Chorin, A.J.

Publication Date
1993-05-01

Lawrence Berkeley Laboratory
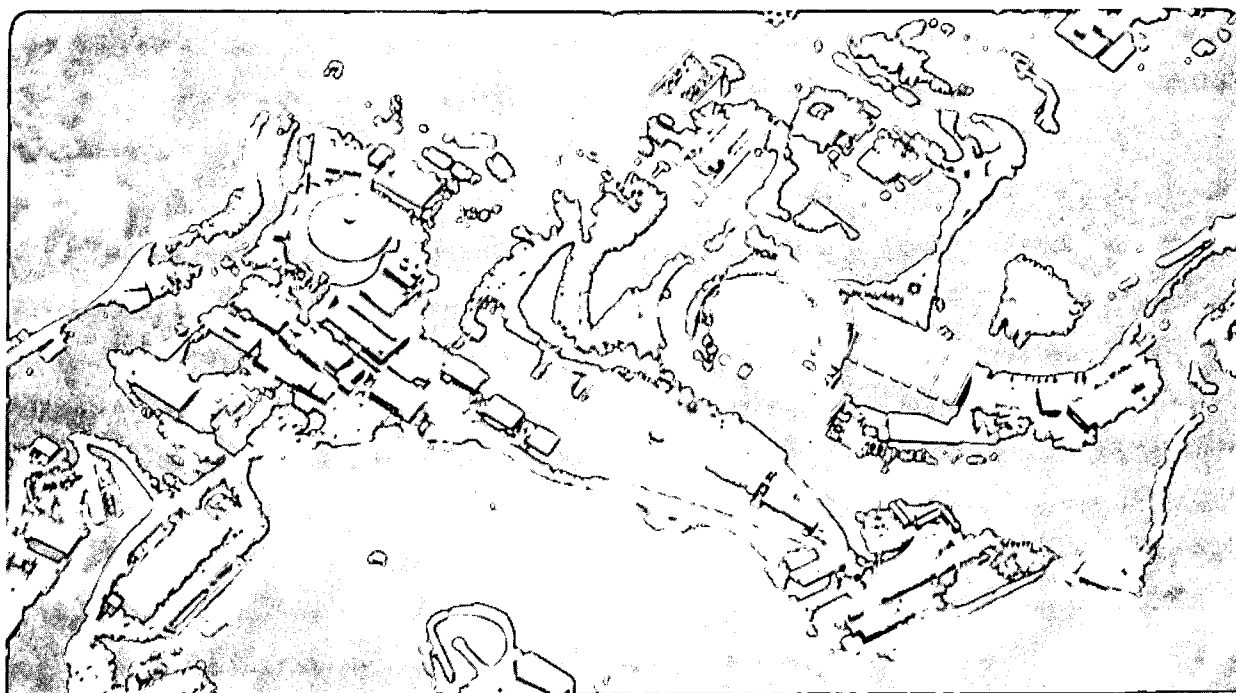## UNIVERSITY OF CALIFORNIA

Physics Division

Mathematics Department

To be presented at the Les Houches Summer School of Theoretical
Physics, Les Houches, France, June 28–July 30, 1993, and to
be published in the Proceedings

Vortex Methods and Vortex Statistics

A.J. Chorin

May 1993

DISCLAIMER

VORTEX METHODS AND VORTEX STATISTICS [1]

Alexandre J. Chorin

Department of Mathematics and Lawrence Berkeley Laboratory
University of California
Berkeley, CA 94720

May 1993

To be presented at
Les Houches Summer School of Theoretical Physics
Les Houches, France
June 28–July 30, 1993

Vortex methods and vortex statistics

Alexandre J. Chorin
Department of Mathematics and Lawrence Berkeley Laboratory
University of California
Berkeley, CA 94720, USA

1. Introduction: what are vortex methods and why do we care?

Vortex methods originated from the observation that in incompressible, inviscid, isentropic flow vorticity (or, more accurately, circulation) is a conserved quantity, as can be readily deduced from the absence of tangential stresses. Thus if the vorticity is known at time $t = 0$, one can deduce the flow at a later time by simply following it around. In this narrow context, a vortex method is a numerical method that makes use of this observation.

However, more generally, viscous flow problems have a Lagrangian, albeit stochastic, representation [C6],[G2],[L4]. Compressible flow has Lagrangian representations [L1]. More generally yet, in many problems there are variables such as charge, stellar or plasma mass, helicity, impulse, chemical species that are transported either passively or modified by known interactions; this transport/modification can be represented by the transport of particles, or polygons, or domain boundaries; by finite elements, finite differences, or boundary integrals. Lagrangian methods have a close resemblance to integral methods (see e.g. [G5]). Aspects of Lagrangian methods, such as particle creation at walls, have found application in non-Lagrangian methods (see e.g. [H5]). Fast summation methods, designed for particle methods, have found uses outside of computational physics.

Even more generally, the analysis of vortex methods leads, as we shall see, to problems that are closely related to problems in quantum physics and field theory, as well as in

harmonic analysis. A broad enough definition of vortex methods ends up by encompassing much of science. Even the purely computational aspects of vortex methods encompass a range of ideas for which vorticity may not be the best unifying theme.

We shall restrict ourselves in these lectures to a special class of numerical vortex methods, those that are based on a Lagrangian transport of vorticity in hydrodynamics by smoothed particles ("blobs") and those whose understanding contributes to the understanding of blob methods. Since excellent recent surveys are available [G7],[P2], the accent will be on recent developments. Blob methods started in the thirties as two-dimensional "point" methods [R7]. By the fifties, it was discovered that "point vortex" methods had drawbacks, and a misinterpretation of the Poincaré recurrence theorem led to the conclusion that the drawbacks could not be remedied (for an analysis, see [K12]). In the late sixties and early seventies, the virtues of smoothing were discovered [C12],[C24] and viscosity and boundaries were added.

The generalization to three dimensions followed soon [C8],[L2],[L3], and was found to be non-unique. Arrows, filaments, dipoles, magnets, all generalize two-dimensional blobs, and we shall compare them below. All three-dimensional inviscid blob methods eventually lose stability; the analysis of that instability requires a deeper understanding of turbulence and contributes to the understanding of quantum fluids.

Are vortex methods good numerical methods? The answer is time-dependent and problem dependent. Vortex methods made possible pioneering investigations of vortex sheets [K10],[K13], high Reynolds number wakes [C4] and various three-dimensional problems involving vortex rings, jets, and wakes (see e.g. [A5],[K6],[M6]). As time progressed,

other methods caught up with some of these applications, but then vortex methods also improved. Various hybrids involving vorticity have appeared in recent years and show great promise (see e.g. [C30],[R9],[W1]). Vortex methods (i.e., "blob" methods) are a very useful part of the panoply of computational fluid mechanics, but do not exhaust it.

I would like however to put some emphasis on a more arcane use of these methods. Vortex methods for inviscid flow lead to systems of ordinary differential equations that can be readily clothed in Hamiltonian form, both in three and two space dimensions, and they can preserve exactly a number of invariants of the Euler equations, including topological invariants. Their viscous versions resemble Langevin equations. As a result, they provide a very useful cartoon of statistical hydrodynamics, i.e., of turbulence, one that can to some extent be analyzed analytically and more importantly, explored numerically, with important implications also for superfluids, superconductors, and even polymers. In my view, vortex "blob" methods provide the most promising path to the understanding of these phenomena.

2. Vortex methods in the plane.

We begin with a quick descriptive version of vortex methods for two-dimensional incompressible flow. Analysis will appear in a later section.

Consider first inviscid flow in the absence of boundaries. The Euler equations take the form

$$\frac{D\xi}{Dt} = 0, \quad \text{div } \mathbf{u} = 0 \tag{1}$$

where $\mathbf{u} = (u_1, u_2)$ is the velocity, $\frac{D}{Dt} \equiv \frac{\partial}{\partial t} + \mathbf{u} \cdot \nabla$, t is the time, $\nabla \equiv \left(\frac{\partial}{\partial x_1}, \frac{\partial}{\partial x_2}\right)$, $\mathbf{x} = (x_1, x_2)$ is the coordinate vector and $\xi = \partial_1 u_2 - \partial_2 u_1$ is the vorticity, where $\partial_i \equiv \frac{\partial}{\partial x_i}$.

3

Define the stream function (scalar vector potential) by $u_1 = -\partial_2 \psi$, $u_2 = \partial_1 \psi$; ψ exists because div $\mathbf{u} = 0$. A quick calculation yields

$$\Delta \psi = -\xi, \quad \Delta \equiv \partial_1^2 + \partial_2^2; \tag{2}$$

make the solution of (2) unique by requiring $|\mathbf{u}| \to 0$ as $|\mathbf{x}| \to \infty$; (2) then yields

$$\psi = - \int G(\mathbf{x} - \mathbf{x}')\xi(\mathbf{x}')d\mathbf{x}',$$

where $G = -\frac{1}{2\pi} \log |\mathbf{x}|$ is Green's function for the Δ operator in two dimensions. Differentiation of ψ yields

$$\mathbf{u} = K * \xi, \tag{3}$$

where $K = (\partial_2 G, -\partial_1 G) = (2\pi|\mathbf{x}|^2)^{-1}(-y, x)^T$, and T denotes a transpose. Note that the kernel in the convolution integral is singular. The trajectory of a particle originally at $\boldsymbol{\alpha}$ satisfies

$$\frac{d\mathbf{x}}{dt}(\boldsymbol{\alpha}, t) = \mathbf{u}(\mathbf{x}(\boldsymbol{\alpha}, t), t) = K * \xi. \tag{4}$$

The integro-differential equation (4) is the starting point for vortex approximations. In a vortex "blob" method, one picks N points $\alpha_1 \cdots \alpha_N$ in the support of the vorticity, and follows their subsequent motion by approximating (4); these trajectories will be denoted by $\tilde{\mathbf{x}}_i(t), \tilde{\mathbf{x}}_i(0) = \boldsymbol{\alpha}_i$ (the tilde will be omitted when there is no risk of confusion). It is natural to approximate the integral by a sum, and useful to modify the singular kernel so that it becomes smooth, $K \to K_\delta = K * \phi_\delta$, where $\phi_\delta = \delta^{-2}\phi(\mathbf{x}/\delta)$, $\int \phi d\mathbf{x} = 1$ (using Hald's formalism [H1]), thus

$$\frac{d\tilde{\mathbf{x}}_i}{dt} = \sum_{j \neq i} \tilde{\xi}_j K_\delta(\tilde{\mathbf{x}}_i - \tilde{\mathbf{x}}_j), \tag{5}$$

where the $\tilde{\xi}_j$ are constants, the approximate values of ξ assigned to the α_j. Good choices for the $\tilde{\xi}_j$ are described e.g. in [A4],[B2],[B6], as well as below for problems with boundaries. The smoothing of K by ϕ removes the singularity in K, and thus ensures that the velocity field remains bounded. More generally, the choice of ϕ controls accuracy, see below. Examples of useful ϕ's are: (i) $\phi = (2\pi|\mathbf{x}|\delta)^{-1}$ for $|\mathbf{x}| \leq \delta$, $\phi = 0$ for $|\mathbf{x}| > \delta$; (ii) $\phi = \pi^{-1}e^{-|\mathbf{x}|^2}$, see more below. The velocity field $\mathbf{u} = \sum K_\delta(\mathbf{x} - \tilde{\mathbf{x}}_j)\tilde{\xi}_j$ is an approximation to the true velocity field; it is also the exact velocity field generated by $\xi = \sum_j \tilde{\xi}_i \phi_\delta(\mathbf{x} - \mathbf{x}_i)$ at time t. A term of the form $\tilde{\xi}_j \phi_\delta(\mathbf{x} - \mathbf{x}_j)$ will be called a vortex blob or vortex for short. If $\phi_\delta = \delta$ (Dirac delta) we recover the old "point" vortex approximation. We assume the reader can solve the ordinary differential equations (5) on a computer, and note that the system (5) is not particularly stiff; Runge-Kutta works fine.

There are very useful Lagrangian approximations of equation (4) other than blob approximations [B13],[R9],[W1]. In particular, suppose supp ξ, the support of ξ, can be approximated by a union of polygons (say, triangles) $Q_1 \cdots Q_N$, with ξ on Q_i approximated by a polynomial P_i. The convolution integrals $K * \tilde{P}_i$, $\tilde{P}_i = P_i$ on Q_i, $\tilde{P}_i = 0$ otherwise, can be expressed in terms of elementary functions and defines everywhere a velocity field that can be used to move the polygons forward. The new vorticity field can be retriangulated efficiently, and the result is an accurate and reliable method. This method is most natural in cases where ξ is piecewise constant, when the polygons can be large.

The Navier-Stokes equations in two space dimensions can be written as

$$\frac{D\xi}{Dt} = R^{-1}\Delta\xi, \quad \text{div } \mathbf{u} = 0, \tag{6}$$

where R is the Reynolds number; we are interested in the case of large R. The inviscid

methods just described can be extended to this case by coupling them to a solution of the heat equation on a moving set of approximation points, see [C30],[F1]. The random vortex method [C6] is based on the observation that equation (6) can be viewed as a Fokker-Planck equation for the stochastic ordinary differential equations

$$d\tilde{\mathbf{x}} = \mathbf{u}\,dt + \sqrt{2/R}\,d\mathbf{w}, \quad \mathbf{u} = K * \xi, \tag{7}$$

where $d\mathbf{w}$ is two-dimensional Brownian motion and $\tilde{\mathbf{x}}(t)$ carried a constant vorticity $\tilde{\xi}$. Equation (7) can be discretized in a straightforward manner; it is a Langevin equation for the vortex system.

Suppose now a boundary is present. If $R^{-1} = 0$, the approximate boundary condition (often $\mathbf{u} \cdot \mathbf{n} = 0$, where $\mathbf{n}$ is a normal to the boundary) is satisfied if G above is replaced by the Green function appropriate to the domain at hand. In practice, all one has to do is add to $\mathbf{u} = K * \xi$ a potential flow $\mathbf{u}_p$ such that their sum satisfies the boundary condition. If $R^{-1} \neq 0$, the condition $\mathbf{u} \cdot \boldsymbol{\tau} = V_\tau$ must also be satisfied, where $\boldsymbol{\tau}$ is tangential to the boundary and V_τ is the tangential velocity of a solid boundary. In principle, all one has to do in this case is create a vortex sheet at the wall, with a strength calculated so as to annihilate unwanted deviations of $\mathbf{u} \cdot \boldsymbol{\tau}$ from its prescribed value. The vorticity in the sheet diffuses into the fluid and participates in the subsequent motion; this process mimics the physical process of vorticity generation.

What is simple in principle is not necessarily so simple in practice. If one calculates with a finite time step Δt, and if at each time step one allows the vorticity to diffuse and be advected, the boundary condition $\mathbf{u} \cdot \boldsymbol{\tau} = V_\tau$ is satisfied exactly only at the beginning and at the end of each step, with local error that is at best $O(\sqrt{\Delta t})$ [C26]. One has to create some

6

device to satisfy the boundary condition continuously. In the context of a blob method, this is done naturally by symmetry. For example, if the boundary is the x_1 axis, with the fluid in the $x_2 > 0$ half-plane, then one can continue the flow to the lower half-plane by the symmetry $\mathbf{u}(x_1, -x_2) = 2V_\tau - \mathbf{u}(x_1, x_2)$, guaranteeing $u_1(x_1, 0) = V_\tau$. Unfortunately, the Navier-Stokes equations are not invariant under this symmetry (consider what happens to $\xi = \partial_2 u_1 - \partial_1 u_2$), but the Prandtl equations $\xi_t + (\mathbf{u} \cdot \nabla)\xi = R^{-1}\partial_2^2\xi$, div $\mathbf{u} = 0$, that approximate them near walls, are invariant. The Prandtl equations have a blob representation [C8], and one can use the Prandtl blobs near walls, in a numerical boundary layer that should be thinner than any physical boundary layer, and then use a standard blob method in the interior.

The problem that remains is the correct matching of boundary blobs with standard blobs. An easy and workable solution is to transfer circulation from one type to the other across some line parallel to the wall, while matching the velocities parallel to the wall. However, as is known from experience with matched asymptotic expansions, high accuracy requires a cleverer match. In particular, one should note that the velocity field induced by a Prandtl blob in its own neighborhood differs substantially from the velocity field induced by a standard blob, and the resulting mismatch of vertical velocities can deplete or overcrowd the vorticity in the transition zone and delay convergence. One would like an overlap between the numerical boundary layer and the interior, and a match of both velocity components. For an appropriate construction, see [R2] and also [B10].

Finally, note that equations (5) can be written in Hamiltonian form. The variable conjugate to the x_1 coordinate of the position of the vortex is the x_2 coordinate of the

position; the Hamiltonian, in the case of point vortices, has the form

$$H = -\frac{1}{4\pi} \sum_i \sum_{j \neq i} \tilde{\xi}_i \tilde{\xi}_j \log |\mathbf{x}_i - \mathbf{x}_j|,$$

with an appropriate smoothing when $\phi_\delta \neq \delta$. H differs from the kinetic energy $\frac{1}{2} \int \mathbf{u}^2 d\mathbf{x}$ by a constant, which is finite if ϕ_δ is smooth.

3. Fast summation.

At first glance, a time step in a blob method with N blobs requires $O(N^2)$ operations, a forbidding number if N is large. It turns out that the calculations require far less effort, typically $O(N \log N)$ operations.

The key observation, as explained by Almgren et al. [A1], is that interactions that can be described by partial differential equations are overwhelmingly local. In particular, interactions described by a Green's function for a Laplacian place a heavy emphasis on what happens when particles are near each other. For overall accuracy, it is enough if nearby interactions are calculated accurately, while distant interactions are calculated in a more global way, for example by conflating series or inverting an approximate Laplacian. Such partitioning schemes can be relatively inexpensive. Examples of algorithms that embody these observations are the local correction method [A1],[A2] the multipole expansion [G5], and other partitioning schemes [B1]. To explain the idea here, we pick a construction that is simple, elegant, and not very well known: Anderson's Poisson integration method [A3]. It can be viewed as a reformulation of the multipole method, and uses ideas developed by Rohklin.

We consider the two-dimensional case (extension to three dimensions is straightforward). Diffusion does not affect the summation. To begin with, we consider point vortices,

8

$\phi_\delta = \delta$; the extension to blobs is trivial. We thus have N point vortices, whose effect we wish to evaluate at N points. For simplicity, we shall write formulas as if the object were to evaluate a stream function ψ; formulas for the velocity can be obtained by differentiation.

Suppose one has M vortices within a circle C of radius a and boundary ∂C, centered at the origin for ease of notation. Remember that two stream functions that are irrotational outside C, have the corresponding velocity fields vanish at infinity, and agree on ∂C, are identical. At a point (r, θ) outside C, ψ is given by

$$\psi(r,\theta) = \kappa \log r + \frac{1}{2\pi} \int_{\partial C} \psi(a,\theta) P(r, \theta') d\theta', \tag{7}$$

where κ is a constant and

$$P(r, \theta) = \left(1 - (a/r)^2\right) / \left(1 - 2(a/r)\cos(\theta - \theta') + (a/r)^2\right)$$

(the Poisson integration formula). The logarithmic term is written explicitly for convenience, and can be incorporated in the integral by adding a constant to $\psi(r, \theta)$. $\psi(a, \theta)$ is determined by the given vortices inside C. If the integral is approximated by a sum with K terms, $K \ll M$, and one wishes to calculate the ψ due to the M vortices at points outside C, then labor is saved. Accuracy for modest K normally requires equidistant integration nodes on C.

A reminder of the derivation of the Poisson formula brings some useful insights. $\psi(r, \theta)$ can be expanded outside C in planar harmonics,

$$\psi(r,\theta) = \kappa \log r + \sum_{k=1}^{\infty} C_k \left(\frac{a}{r}\right)^k e^{ik\theta};$$

on $r = a$, this series reduces to a Fourier series, and thus the C_k can be found. A summation and an interchange of summation and integration yields (7). Note:

(i) Numerical integration mishandles high wave numbers, and thus for numerical purposes the expansion in planar harmonics need only be carried up to a finite number of terms. Summation and exchange of limits then produce a new kernel P_K that is better conditioned than P.

(ii) The error in the expansion, and thus in the use of the Poisson formula, depends only on $\psi(r,\theta)$ and on r/a, and is therefore scale invariant.

It is obvious that data on circles of one size can be used to produce values of ψ on larger circles that surround the smaller ones. One can thus produce values of ψ on a growing family of circles, each level using distant large circles or nearly small circles as needed for accuracy. If $\phi_\delta \neq \delta$, the support of ϕ_δ sets a lower bound on the radii of the circles; the results is an $O(N \log N)$ algorithm.

For more detail, see [A3]; the general structure of fast summation algorithms is discussed in [K1].

4. The convergence of vortex methods.

We now present a brief sketch of the convergence theory for vortex methods [B5],[B6],[C29],[H1],[H2],[R1], in the simplest case: two dimensions, $R^{-1} = 0$, ξ of compact support and no boundaries. The theory presented should be sufficient to illustrate the following points: (i) The error in vortex methods is primarily due to the error in the evaluation of the convolution integrals (4), and (ii) Accuracy depends on the properties of the smoothing ϕ, and can be enhanced by imposing on it certain moment conditions. The theory here should also give some of the flavor of the extensive and elegant body of work that has arisen in this context. The presentation here follows in the main references

10

[A4],[C28].

Remember that the kernel K has been smoothed in the form: $K \to K_\delta$, $K_\delta = K * \phi_\delta$, $\phi_\delta = \delta^{-2}\phi(\mathbf{x}/\delta)$, $\int \phi d\mathbf{x} = 1$. Suppose ϕ is smooth enough (for precise requirements, see the references) and in addition, satisfies $\int \mathbf{x}^\alpha \phi(\mathbf{x})d\mathbf{x} = 0$, where $\mathbf{x}^\alpha = x_1^{\alpha_1} x_2^{\alpha_2}$, $|\alpha| = \alpha_1 + \alpha_2$, and $0 < |\alpha| \le p - 1$ for some p, i.e., the moments of ϕ up to order $p - 1$ vanish. The vortex method is written in the form (5): $d\tilde{\mathbf{x}}_i/dt = V_i(\tilde{\mathbf{x}})$, where $V_i(\mathbf{x}) = \sum_j \tilde{\xi}_j K_\delta(\mathbf{x}_i - \mathbf{x}_j)$.

Consider N blobs initially at $\boldsymbol{\alpha}_j$, $j = 1, \ldots, N$, where the $\boldsymbol{\alpha}_j$ are nodes of a regular square mesh of mesh size h placed on the support of ξ, and let $\tilde{\xi}_j = \xi(\boldsymbol{\alpha}_j)$. Let $\mathbf{x}_j(\boldsymbol{\alpha}_j, t)$ be the true trajectories issuing from the $\boldsymbol{\alpha}_j$, and $\tilde{\mathbf{x}}_j(\boldsymbol{\alpha}_j, t)$ the computed trajectories. Let $e_j(t) = x_j(\boldsymbol{\alpha}, t) - \tilde{x}_j(\boldsymbol{\alpha}, t)$, and for the sake of brevity, omit the subscript j from now on. $\dot{e} = \frac{de}{dt}$ satisfies

$$
\begin{aligned}
\dot{e} &= \dot{\mathbf{x}} - V(\tilde{\mathbf{x}}) \\
&= e_m + e_d + e_s,
\end{aligned}
$$

with

$$
\begin{aligned}
e_m &= \int K(\mathbf{x} - \mathbf{x}')\xi(\mathbf{x}')d\mathbf{x}' - \int K_\delta(\mathbf{x} - \mathbf{x}')\xi(\mathbf{x}')d\mathbf{x}' \\
e_d &= \int K_\delta(\mathbf{x} - \mathbf{x}')\xi(\mathbf{x}')d\mathbf{x}' - \sum_j K_\delta(\mathbf{x} - \mathbf{x}_j)\tilde{\xi}_j \\
e_s &= \sum_j K_\delta(\mathbf{x} - \mathbf{x}_j)\tilde{\xi}_i - \sum_j K_\delta(\tilde{\mathbf{x}}_i - \tilde{\mathbf{x}}_j)\tilde{\xi}_j.
\end{aligned}
$$

e_m is the "moment error" which arises because $K \to K_\delta$ (the origin of the name will become clear in a moment); e_d is the discretization error which results from the replacement of the integral by a sum; e_s is the stability error which arises because the sum is evaluated on the computed rather than the exact location of the blobs. We shall now estimate these errors, noting that any integration over $\mathbf{x}$ or $\mathbf{x}'$ can be replaced by an integration over $\boldsymbol{\alpha}$ or $\boldsymbol{\alpha}'$ (the Jacobian of the map $\boldsymbol{\alpha} \to \mathbf{x}$ being 1 by incompressibility); the grid in the integrations

11

can thus be viewed as being regular even when the blob distribution has ceased to be regular as a result of the motion.

We defined $e_m = K * \xi - K_\delta * \xi$; Thus

$$\hat{e}_m(\mathbf{k}, t) = (\hat{K} - \hat{K}_\delta)\hat{\xi},$$

where $\mathbf{k}$ is the variable conjugate to $\mathbf{x}$ and $\hat{\ }$ denotes a Fourier transform;

$$\hat{e}_m = \hat{K}(1 - \hat{\phi}_\delta)\hat{\xi},$$
$$= \hat{K}\hat{\xi}\left(\hat{\phi}(0) - \hat{\phi}(\delta\mathbf{k})\right),$$

since $1 = \int \phi d\mathbf{x} = \hat{\phi}(0)$. The moment condition guarantees that the derivatives of orders up to $p-1$ of $\hat{\phi}$ are zero, and straightforward manipulation yields $\| e_m \|_{L^1} \leq$ constant $\cdot \delta^p$.

To estimate e_d, we shall first exhibit some inequalities which prove the high order accuracy of trapezoidal rule integration for sufficiently smooth integrands. Elementary considerations show that if $\mathbf{i} = (i_1, i_2)$ is a pair of integers, $\mathbf{i} = 0$ if $i_1 = 0$, $i_2 = 0$, and $\| \mathbf{i} \| = \max(|i_1|, |i_2|)$, then for $L \geq 3$, $\sum_{\mathbf{i} \neq 0} \| \mathbf{i} \|^{-L} \leq 16$. Suppose $g = g(x_1, x_2) \in C_0^r$, and define $\| g \|_r = \max(\| \partial^r g \|_{L^1})$ (the maximum of the L^1 norms of all the derivatives of g up to order r). Then, for $r \geq 3$,

$$\left| \sum_{\mathbf{i}} g(\mathbf{i}h) - \int g(\mathbf{x})dx \right| \leq \frac{12}{(2\pi)^r} \| g \|_r h^r$$

(trapezoidal rule integration is very accurate). Indeed, by the Poisson summation formula [D3],

$$h^2 \sum_{\mathbf{i}} g(\mathbf{i}h) = \sum_{\mathbf{i}} \hat{g}(\mathbf{i}/h),$$

where $\hat{g}$ is the Fourier transform of g. Therefore,

$$\left| h^2 \sum_{\mathbf{i}} g(\mathbf{i}h) - \int g(\mathbf{x})dx \right| = \left| \sum \hat{g}(\mathbf{i}h) - \hat{g}(0) \right| = \left| \sum_{\mathbf{i} \neq 0} \hat{g}(\mathbf{i}/h) \right|.$$

12

Also, $|\hat{g}| \leq \int |g(\mathbf{x})| d\mathbf{x}$, and $\widehat{\partial^\alpha g}(\mathbf{k}) = (2\pi i)^{|\alpha|} k^\alpha \hat{g}(k)$, where $\partial^\alpha = \partial_1^{\alpha_1} \partial_2^{\alpha_2}$, $|\alpha| = \alpha_1 + \alpha_2$, and $k^\alpha = k_1^{\alpha_1} k_2^{\alpha_2}$; thus

$$|(2\pi)^r k^r \hat{g}| \leq \int |\partial^r g| d\mathbf{x} \leq \| g \|_r .$$

Then

$$|\hat{g}(\mathbf{k})| \leq \frac{\| g \|_r}{(2\pi)^r} \frac{1}{\| \mathbf{k} \|^r},$$

and for $r \geq 3$,

$$\left| \sum_{\mathbf{i} \neq 0} \hat{g}(i/h) \right| \leq \left| \frac{\| g \|_r}{(2\pi)^r} \sum_{\mathbf{i} \neq 0} \| \mathbf{i}/h \|^{-r} \right| \leq \frac{16}{(2\pi)^r} \| g \|_r h^r .$$

To estimate e_d, all we need is an estimate for the derivatives of $K_\delta = K * \phi_\delta$. K_δ has as many derivatives as ϕ has, and if ϕ has L derivatives, a straightforward analysis yields at finite time T:

$$\max_{0 \leq t \leq T} \| e_d \|_{L^\infty} \leq \text{constant} \cdot \left(\frac{h}{\delta} \right)^L \cdot \delta.$$

We omit the analysis of e_s, which can be bounded in such a way that the over-all error is bounded by a constant times $(\| e_d \| + \| e_m \|)$; thus

$$\| \text{error} \|_{L^1} \leq \text{constant} \left(\delta^p + \left(\frac{h}{\delta} \right)^L \delta \right).$$

(Note the usefulness of δ.) If L is large enough, one can choose $h/\delta < 1$ (thus making the blobs overlap) so that the error in the trajectories of the blobs is close to $O(h^p)$. We omit the discussion of how one goes from trajectory error to other measures of the error, and how one accounts for the effects of time discretization. For error estimates in the presence of viscosity or in three dimensions, see the references.

The key to accuracy (or more precisely, to local accuracy, see below) in blob methods is to satisfy the moment conditions $\int \mathbf{x}^\alpha \phi d\mathbf{x} = 0$ for α as large as possible. An appropriate

13

choice of ϕ can produce spectral accuracy [H2]. A popular choice of ϕ is the Beale-Majda fourth order $(p = 4)$ core $\phi_4 = e^{-r^2} - \frac{1}{2}e^{-r^2/2}$; for a derivation, see [B6], where the three-dimensional case is discussed as well.

The error in blob method does grow in time. One factor in this exponential growth is the growing irregularity of the blob distribution and the resulting growth in the derivatives that enter the error in a trapezoidal rule. This growth can be remedied by periodic rezoning (see e.g. [N4]). By construction, the polygon methods mentioned above perform a rezoning at each time step, and as a result the errors they produce often grow less rapidly.

Other limitations on long-time accuracy will be discussed in the next few sections.

5. Vortex methods in three dimensions.

In three space dimensions, vortex methods are a little more difficult to formulate because the vorticity is now a divergence-free vector whose magnitude changes in time. The Euler equations take the forms

$$\partial_t \boldsymbol{\xi} + (\mathbf{u} \cdot \nabla)\boldsymbol{\xi} = -(\boldsymbol{\xi} \cdot \nabla)\mathbf{u}, \tag{8}$$

$$\text{div } \mathbf{u} = 0,$$

where $\boldsymbol{\xi} = \text{curl } \mathbf{u}$ is the vorticity. The definition of $\boldsymbol{\xi}$ can be inverted and yields, as in equation (3),

$$\mathbf{u} = K * \boldsymbol{\xi}, \tag{9}$$

where the kernel K is now $K = - \left(4\pi|\mathbf{x}|^3\right)^{-1} \times$, $\times$ denoting a cross-product. Equation (9) is known as the Biot-Savart law. In the *filament* method, one writes

$$\boldsymbol{\xi} = \sum_i \boldsymbol{\xi}_i$$

14

where the supports of the $\boldsymbol{\xi}_i$ are tubes of small cross-section tangent to the vorticity field ("vortex filaments"). $\mathbf{u}$ is approximated by $K_\delta * \boldsymbol{\xi} = \sum_i K_\delta * \boldsymbol{\xi}_i$, where K_δ is a smoothed kernel $K_\delta = K * \phi_\delta$, and the integration along a filament is approximated by a sum. The non-constancy of $\mathbf{u}$ along the support of $\boldsymbol{\xi}_i$ automatically takes care of vortex stretching (the effect of the right-hand-side of equation (8)). High order methods can be obtained through a good choice of ϕ in $\phi_\delta = \delta^{-3}\phi(\mathbf{x}/\delta)$ [B5],[G4]. With $\phi_\delta \neq \delta$, and the integral replaced by a sum, and $\mathbf{u} \neq K * \boldsymbol{\xi}$, and thus div $\boldsymbol{\xi} \not\equiv 0$, but one can make div $\boldsymbol{\xi}$ be small enough for practical purposes. Vortex stretching is a strong effect, and as it takes hold, approximation points must be added to the filaments [C10],[K5]. Practical applications can be found in [C10],[G1],[K7],[K14],[L3].

The problem with the filament method is that it is not obvious how to couple it to a diffusion method; furthermore, there is little experience in producing filament at walls (but see [S6]). A way around these difficulties is to approximate each filament by a sum of vortex *segments*, (also know as "sticks", "arrows" and "vortons"), and then proceed as if the segments were independent, relying on convergence to make div $\boldsymbol{\xi} \sim 0$, see [B4],[C8]. Diffusion and boundary conditions can then be dealt with quite easily. On the other hand, it is very important for long-time accuracy that div $\boldsymbol{\xi}$ be very small [B14], and one may have to filter out the non-divergence-free part of the vorticity field at frequent intervals. For a recent review, see [W5]. There is a substantial recent Russian literature on segment methods with $\phi_\delta = \delta$ (no smoothing), for reasons that are hard to fathom.

An interesting alternative to segment methods that deals with "local" elements, enforces div $\boldsymbol{\xi} = 0$ and can be coupled to diffusion has been introduced by Buttke [B14],[B15];

the computational elements are small vortex loops [O1],[R4],[R8], appropriately smoothed. At $t = 0$, pick a scalar function q and consider the equations of motion for $\mathbf{m} = \mathbf{u} + \text{grad } q$. $\mathbf{m}$ is a "magnetization", or "impulse density", or "dipole density", and q being arbitrary at $t = 0$, is clearly not unique. However, if P is the operator that projects arbitrary vector fields on their divergence-free part that is tangential to boundaries (P is well defined [C25]), and if $\mathbf{m}$ remains the sum of $\mathbf{u}$ and a gradient at later times, then $\mathbf{u} = P\mathbf{m}$ is uniquely defined. Let $\mathbf{m} = (m_1, m_2, m_3)$. One can readily check that the equations

$$\frac{Dm_i}{Dt} = -m_j \partial_i u_j + R^{-1} \Delta m_i, \quad \mathbf{u} = P\mathbf{m}, \tag{10}$$

produce a velocity field that is equal to the one produced by the Navier-Stokes equations with the same data. If $R^{-1} = 0$, (10) is equivalent to Euler's equations.

The freedom in choosing q can be put to very good use. Suppose the vorticity $\boldsymbol{\xi}$ has compact support. The velocity field $\mathbf{u}$ has support in a set that extends to infinity. Let H be the convex hull of the support of $\boldsymbol{\xi}$. Outside H, $\mathbf{u}$ can be written as $\mathbf{u} = -\text{grad } \tilde{q}$, since the complement of H is simply connected. At $t = 0$, set $q = \tilde{q}$. The corresponding $\mathbf{m}$ has support in H and has thus been "localized". If one then writes $\mathbf{m} = \sum \mathbf{m}_j$, with the supports of the $\mathbf{m}_j$ small and in H ($\mathbf{m}_j$ is a "magnet"), then one obtains a representation of the flow field by a sum of localized particles. The vorticity $\boldsymbol{\xi} = \text{curl } \mathbf{m}$ satisfies div $\boldsymbol{\xi} = 0$; $\mathbf{u}$ can be obtained by $\mathbf{u} = K * \boldsymbol{\xi}$. If $\mathbf{x}_i$ is the "center" of the i-th magnet, then $d\mathbf{x}_i/dt = \mathbf{u} = \sum_j K * (\text{curl } \mathbf{m}_j)$. Equation (10) yields an evolution equation for $\mathbf{m}$; $K \to K_\delta$ yields accuracy. If $R^{-1} = 0$, the equations form a Hamiltonian system. If $R^{-1} \neq 0$, diffusion can be handled as in two dimensions.

A comparison of $\mathbf{u} = K * \text{curl } \mathbf{m}$, where $\mathbf{m}$ is one magnet, with the velocity field induced

16

by a small vortex loop at a large distance, shows that the magnetization $\mathbf{m}$ representation is in fact a representation in terms of small vortex loops. Consider a large-scale vortex Γ; to construct an $\mathbf{m}$ representation one finds a (non-unique) surface Σ that spans Γ, and one places magnets $\mathbf{m}$ on Σ so that they are normal to Σ and have magnitudes $|\mathbf{m}| = \frac{1}{2}|\Gamma||d\Sigma|$, where $|\Gamma|$ is the circulation in the vortex loop Γ and $d\Sigma$ is the surface element on Σ. It is easy to check that $\mathbf{m}$ remains orthogonal to Σ as both are evolved by the flow map. This construction points out a problem with the $\mathbf{m}$ representation: A vortex loop will eject fluid to its rear and thus Σ will balloon; as its area increases so does $\sum |\mathbf{m}_j|$; as a result the time steps may become small and the calculation expensive. Appropriate remaps to remedy this problem have been considered by Cortez [C27]. The magnetization representation has not yet been tested as a sufficient number of examples for firm conclusions about its usefulness to be drawn. If $R^{-1} = 0$, one can verify that the equations of motion of N magnets have Hamiltonian form.

All inviscid three-dimensional vortex representations eventually run into the "folding" problem. As a flow evolves, vortex lines stretch; as they stretch they must fold, or else energy conservation cannot be obeyed; folding creates the necessary cancellations between the velocity fields induced by the stretching vortex lines. Stretching and folding are real physical processes that occur in fluid flows [C11],[C18],[C21]; their numerical versions are not necessarily faithful to reality. The explosive growth in stretching and folding that is characteristic of vortex methods can limit their usefulness. The reasons for this growth and the methods that control it can be understood in a statistical mechanics context that we shall now develop. The analysis also has direct applications to the analysis of vortex

motion in turbulent flow and in quantum fluids.

6. Statistical mechanics of vortices in the plane.

We start the statistical analysis by considering N vortices in the bounded region $\mathcal{D}$ in two dimensions. The entropy S of the system is the logarithm of the density of its states (the Boltzman constant can be set equal to 1 by using appropriate units). The temperature T is defined by $T^{-1} = dS/d\langle E \rangle$, where $\langle E \rangle$ s the average of the energy E. If the system has states labelled by a parameter s, then $S = -\sum_s P_s \log P_s$, where P_s is the probability of the state s and the sum is to be interpreted as an integral when the states form a continuum. In the canonical ensemble, $P_s = Z^{-1} \exp(-E/T)$, where $E = E(s)$ is the energy of the state labelled by s and Z is a normalizing constant, the "partition function" $Z = \sum P_s$.

One is used to having $T > 0$, but this inequality is not a law of nature. One can perfectly well imagine systems such that for $\langle E \rangle$ moderate there are many ways of arranging their components so that the energy adds up to $\langle E \rangle$ but for $\langle E \rangle$ large there are only a few ways of doing so. Then the derivative $dS/d\langle E \rangle$ is negative for $\langle E \rangle$ large enough and T is negative. This situation will indeed occur for vortex systems. If $T > 0$ low energy states have a high probability, and if $T < 0$ high energy states have a high probability.

Suppose one takes two systems, each separately in equilibrium, one with energy E_1 (we drop the brackets) and entropy S_1, the other with energy E_2 and entropy S_2. Suppose one joins them; the resulting union has energy $E_1 + E_2$ and is not necessarily in equilibrium. Its entropy, initially $S = S_1 + S_2$, will increase in time t. Then

$$\frac{dS}{dt} = \frac{dS_1}{dt} + \frac{dS_2}{dt} = \frac{dS_1}{dE_1}\frac{dE_1}{dt} + \frac{dS_2}{dE_2}\frac{dE_2}{dt} > 0,$$

while energy is conserved:

$$\frac{dE_1}{dt} + \frac{dE_2}{dt} = 0.$$

Therefore

$$\frac{dS}{dt} = \left(\frac{dS_1}{dE_1} - \frac{dS_2}{dE_2}\right)\frac{dE_1}{dt} = \left(\frac{1}{T_1} - \frac{1}{T_2}\right)\frac{dE_1}{dt}.$$

Suppose $T_2 > T_1$, both positive; then $\frac{dE_1}{dt} > 0$, i.e., energy moves from the hotter body to the colder body. Now suppose $T_2 < 0$. It still follows that $\frac{dE_1}{dt} > 0$, i.e. a body with negative temperature is "hotter" than a body with positive temperature. Negative temperatures are above $T = \infty$, rather than below absolute zero. Further, the canonical formula shows that $T = -\infty$ is indistinguishable from $T = +\infty$; $|T| = \infty$ is the boundary between $T < 0$ and $T > 0$. In terms of $\beta = T^{-1}$, temperature increases as β varies from infinity to zero through positive values, and then from zero to minus infinity through negative values.

Consider a collection of N vortices of small support occupying a finite portion $\mathcal{D}$ of the plane, of area $A = |\mathcal{D}|$ (see [E1]). The area can be made finite by surrounding it with rigid boundaries, in which case the vortex Hamiltonian must be modified through the addition of immaterial smooth terms; alternatively, one can confine the vortices to a finite area initially and conclude that they will remain in a finite area, because the center of vorticity $\mathbf{X} = \Sigma\tilde{\xi}_i\mathbf{x}_i/\Sigma\tilde{\xi}_i$, $\mathbf{x}_i$ = positions of the vortices, and the angular momentum $\Sigma\tilde{\xi}_i^2|\mathbf{x}_i - \mathbf{X}|^2$ are invariant. For the moment, consider inviscid flow with all the $\tilde{\xi}_i = 1$. The entropy of this system is

$$S = -\int_{\mathcal{D}^N} f(\mathbf{x}_1, \ldots, \mathbf{x}_N)\log f(\mathbf{x}_1, \ldots, \mathbf{x}_N)d\mathbf{x}_1 d\mathbf{x}_2 \cdots d\mathbf{x}_N,$$

where f is the probability that the first vortex is in a small neighborhood of $\mathbf{x}_1$, the second in a small neighborhood of $\mathbf{x}_2$, etc. The energy of this system is $E = H + B$, where H is the two-dimensional vortex Hamiltonian and B is an appropriate constant. The entropy is maximum when

$$f = \text{constant} = A^{-N}.$$

The corresponding energy is

$$\langle E \rangle = \langle E_c \rangle = -\frac{1}{4\pi} N(N-1) \int_{\mathcal{D}} d\mathbf{x} \int_{\mathcal{D}} d\mathbf{x}' \log |\mathbf{x} - \mathbf{x}'| + B.$$

Clearly, one can produce a larger $\langle E \rangle$ by bunching vortices together, and thus $T^{-1} = dS/dE < 0$ for $E > \langle E_c \rangle$. This is Onsager's observation. If $T > 0$, the Gibbs factor $\exp(-E/T)$ gives a high probability to low energy states, and if $T < 0$, high energy states are favored; the latter are produced by bunching together vortices, forming large, concentrated vortex structures. The $f = \text{constant}$ state is the $|T| = \infty$ boundary between $T < 0$ and $T > 0$. The T introduced here has no connection whatsoever with the molecular temperature of the underlying fluid; in incompressible flow, the molecular degrees of freedom and the vortex variables are insulated from each other.

To give this argument a more quantitative form, we turn to the elementary combinatorial method [J1]. We assume there are N vortices. N^+ vortices have strength $\tilde{\xi} = 1$, N^- have $\tilde{\xi} = -1$, $N^+ + N^- = N$. We divide $\mathcal{D}$ into M boxes of area h^2, with n_i^+ positive and n_i^- negative vortices in each. The corresponding probability (= multiplicity) W is

$$W = \left(\frac{N^+!}{n_1^+! \ldots n_M^+!} \right) \left(\frac{N^-!}{n_1^-! \ldots n_M^-!} \right) h^{2N}.$$

To a good approximation, the entropy is $S = \log W$ (for the conditions under which this is true, see e.g. [E1],[C21]). To obtain an equilibrium, S is to be maximized subject to the

constraints $\Sigma n_i^+ = N^+$, $\Sigma n_i^- = N^-$, and

$$E = \frac{1}{2} \sum_i \sum_{j \neq 1} (n_i^+ - n_i^-) G_{ij} (n_j^+ - n_j^-) = \text{constant},$$

where $G_{ij} = -\frac{1}{2\pi} \log |\mathbf{x}_i - \mathbf{x}_j| + B$, $\mathbf{x}_i$ is in the i-th box, $\mathbf{x}_j$ is in the j-th box, and B is a constant. This E approximates the energy of a vortex system. The maximization of S produces a thermal equilibrium and leads to the equations

$$\begin{aligned}
\log n_i^+ + \alpha^+ + \beta \sum_j G_{ij} (n_j^+ - n_j^-) &= 0, \\
\log n_i^- - \alpha^+ + \beta \sum_j G_{ij} (n_j^+ - n_j^-) &= 0,
\end{aligned} \tag{11}$$

where $\alpha^+, \alpha^-, \beta$ are Lagrange multipliers. A little algebra yields

$$\begin{aligned}
n_i^+ - n_i^- = \quad &\exp\left(-\alpha^+ - \beta \sum_j G_{ij}(n_j^+ - n_j^-)\right) \\
- \quad &\exp\left(-\alpha^- + \beta \sum_j G_{ij}(n_j^+ - n_j^-)\right),
\end{aligned}$$

for $i = 1, \ldots, M$. Let $h \to 0$ so that $n_i^+ - n_i^- \to \xi(\mathbf{x}) h^2 = \xi(\mathbf{x}) dx$, $(\exp(-\alpha^-))/h^2 \to d^-$, and $\Sigma G_{ij}(n_i^+ - n_i^-) \to \int G(\mathbf{x} - \mathbf{x}') \xi(\mathbf{x}') d\mathbf{x}'$, where $G(\mathbf{x}) = -\frac{1}{2\pi} \log |\mathbf{x}| + B$. Equations (11) converge to

$$\xi(\mathbf{x}) = d_+ \exp\left(+\beta \int G(\mathbf{x} - \mathbf{x}')\xi(\mathbf{x}')d\mathbf{x}'\right) + d_- \exp\left(-\beta \int G(\mathbf{x} - \mathbf{x}')\xi(\mathbf{x}')d\mathbf{x}'\right)$$

where d_+, d_- are appropriate normalization coefficients.

Let ψ be the stream function, $u_1 = -\partial_2 \psi$, $u_2 = \partial_1 \psi$; an easy calculation gives $\Delta \psi = -\xi$, $\Delta = $ Laplace operator and $\psi = -\int G(\mathbf{x} - \mathbf{x}')\xi(\mathbf{x}')d\mathbf{x}'$. Thus,

$$-\Delta \psi = \xi(\mathbf{x}) = d_+ e^{-\beta \psi} - d_- e^{\beta \psi}. \tag{12}$$

This is the Joyce-Montgomery equation. In a periodic domain one can set $\psi = 0$ on the boundary of a period; $N^+ = N^- = N/2$, $d_+ = d_- = d$. Then

$$2d = \frac{N}{\int d\mathbf{x} e^{\beta \psi}},$$

$$-\Delta\psi(\mathbf{x}) = \xi(\mathbf{x}) = d\sinh\beta\psi(\mathbf{x}).$$

If $N^+ = N$, $N^- = 0$, then $d_- = 0$, $d^+ = N/Z$, $Z = \int_D e^{-\beta\psi}d\mathbf{x}$, and

$$-\Delta\psi = \xi(\mathbf{x}) = \frac{N}{Z}\exp\left(\beta\psi(\mathbf{x})\right).$$

In either case, ξ is a function of ψ. The Euler equation is

$$\partial_t\xi = -u_1\partial_1\xi - u_2\partial_2\xi$$
$$= (\partial_2\psi)(\partial_1\xi) - (\partial_1\psi)(\partial_2\xi) = J(\psi,\xi),$$

where $J = $ Jacobian of ξ, ψ which is zero when $\xi = \xi(\psi)$. The resulting average flow is a stationary (time-independent) solution of the Euler equation, with macroscopic motion, as expected when $\beta < 0$. Appropriate forms of equation (12) can be derived, in which the limit $N \to \infty$ can be easily taken [E1],[K3],[M9].

It should be emphasized that the ξ we have calculated is not only a specific solution of Euler's equation, but more importantly it is the stationary average density of the vorticity. Specific flows may depart from this average, but one expects the departure to be small.

For $\beta \geq 0$ and for $-8\pi N < \beta < 0$ equation (12) can be shown to have solutions. In the latter case the solutions are non-unique; the solutions have multiple peaks; the solution that maximizes the entropy has a single sharp but smooth peak. For $\beta < -8\pi N$ (i.e., "hotter" than $T = -1/8\pi N$), the Joyce-Montgomery equation with $\xi \geq 0$ has no classical solution and in fact does not describe reasonable physics.

Statistical equilibria are of interest only if they are reached from most initial data. There is strong evidence, mainly numerical, that the two-dimensional equilibria constructed above are in fact reached. Some general statements can be made about the relaxation to equilibrium, and some equations remain open.

22

Suppose one starts from initial data that consist of two patches of vorticity, say $\xi = 1$ in sets C_1, C_2, both bounded, C_1, C_2 disjoint, and $\xi = 0$ elsewhere. Since vorticity is merely transported by the fluid motion, one has to imagine a process by which the vorticity in the patches is redistributed so as to match ξ_∞, the solution of the one-sign Joyce-Montgomery equation (12). One can imagine that the boundaries of C_1, C_2 sprout filaments, as in the convergence of subsets of the constant energy surface to the microcanonical ensemble; the resulting filaments could reorganize so as to approximate ξ_∞ on a sufficiently crude scale.

The filamentation of the boundary should lower the energy. Indeed, if a small vortex patch is broken into two halves that are pulled apart, the energy goes down; two vortices of strength $\tilde{\xi} = 1$ each, near each other, act as one vortex of strength 2, whose energy is four times that of one of them; two vortices of strength 1 far from each other have an energy that is the sum of their individual energies. To make up for the loss of energy in filamentation the two patches have to approach each other. This process of simultaneous filamentation and consolidation is well documented numerically. Similarly, one expects a non-circular patch to become nearly circular with a halo of filaments, the whole approximating ξ_∞ on a rough scale. Even a circular patch with non-constant ξ, increasing from its center outward, can reorganize its vorticity so that filaments shoot off while energy is being conserved. On the other hand, a patch with ξ decreasing as one moves away from the center is stable, and belongs to the set of initial data that do not approach ξ_∞; such a patch of course does in itself constitute a rough version of ξ_∞.

This process of simultaneous filamentation and consolidation can be deduced from the invariance of the energy and the enstrophy in spectral form: $\int E(k)dk = $ constant,

$\int k^2 E(k) dk = \text{constant}$, where $E(k)$ is the energy spectrum. If some energy moves towards the large k's (small scales), then even more energy must move towards the small k's (large scales). On the whole, there is an energy "cascade" toward the small k's.

If the initial ξ is complicated, and has many maxima and minima, one can imagine, and indeed see on the computer, a process of progressive curdling, in which nearly circular patches that look locally like ξ_∞ first form on small scales, then slowly migrate towards each other and consolidate if viewed on a crude enough scale. The curdles can never truly merge, since the flow map is one-to-one. At each stage of this curdling the nearly circular patches are nearly independent, with whatever correlations their locations have manifesting itself only on large scales. The flow can then be approximated as $\Sigma \eta_i \xi_\infty(\mathbf{x} - \mathbf{x}_i)$, $\eta_i =$ random coefficients. The energy spectrum is approximately proportional to $|\mathbf{k}|^2 |\hat{\xi}_\infty(\mathbf{k})|^2$, where $\hat{\xi}_\infty$ is the Fourier transform of $\xi_\infty(\mathbf{x})$, and is a property of each curd individually. One then has local equilibria slowly consolidating into larger equilibria.

This successive curdling picture provides a suggestion as to what happens in the presence of shear or in complex geometries. In three space dimensions the "universal" aspects of turbulence appear on small scales, and one can readily imagine that arbitrary large scale structures have "universal" small scale features. Here, in two dimensions, the universal structures grow to large scales, and an imposed shear or an imposed boundary mass interferes with them. It is readily imagined however that the curdling process will simply stop when it ceases to be compatible with the conditions imposed on the problem.

Note that if ϕ_δ in the two-dimensional vortex method is identified with ξ_∞, then the vortex method can be reinterpreted as a model of two-dimensional turbulence, in which

the smallest scales have reached equilibrium. Indeed, this is how the ϕ_δ in [C5,[C6] was chosen.

One can wonder about the effect of a small viscosity ν on the processes just described. To the extent that the effect of viscosity is to smear the small scales, and as long as the time it takes to reach equilibrium is small compared to the time scale of viscous decay, the picture above should be unaffected. One could say a little more: suppose the effect of viscosity is approximated by Brownian motion (equation (7)). The Brownian motion can be thought of as being generated by the bombardment of the vortices by the molecules of an ambient fluid at a temperature ν. The effect of the bombardment that has just been imagined is to couple weakly the "fluid" at the temperature ν with the vortex system, and if $\nu < T =$ vortex temperature, to reduce the latter. If $T < 0$, the cooling of the vortex system brings one closer to the $|T| = \infty$ equidistribution solution, in agreement with the intuitive idea that random pushes should interfere with the formation of concentrated vortices. After a long enough time one may end up with $\xi =$ constant.

7. Statistics of vortex filaments in three dimensions.

We now turn to the three-dimensional analogues of the constructions of the previous section. In three dimensions, vortex filaments are extended objects, more like polymers than like particles; vortex stretching is important, and only a statistically steady state can be expected as the time $t \to \infty$. To make the presentation easy, we consider a single vortex filament (a tight bunch of integral lines of the vorticity field) in a dilute "suspension" of such filaments; more general situations are considered in [C18],[C21].

Suppose our filament can be covered by N nearby circular cylinders, each of length

$h > 0$. Endow the filament with an energy

$$E = \frac{\Gamma^2}{8\pi} \sum_i \sum_{j \neq i} \frac{\mathbf{t}_i \cdot \mathbf{t}_j}{|i - j|} \tag{13}$$

where $\mathbf{t}_i$ is a vector of length h originating at the center of the i-th cylinder, $|i - j|$ is the distance between the i-th and j-th cylinders, and Γ is the circulation of the vortex. Equation (13) is the discrete analogue of the Lamb expression for the energy

$$E = \frac{1}{2} \int \mathbf{u}^2 d\mathbf{x} = \frac{1}{8\pi} \int d\mathbf{x} \int d\mathbf{x}' \frac{\boldsymbol{\xi}(\mathbf{x}) \cdot \boldsymbol{\xi}(\mathbf{x}')}{|\mathbf{x} - \mathbf{x}'|}.$$

The vortex is self avoiding: $|\mathbf{x} - \mathbf{x}'| \neq 0$ for $\mathbf{x} \in$ the i-th cylinder, $\mathbf{x}' \in$ the j-th cylinder.

Assume that each configuration C of the vortex has probability $P(C) = Z^{-1} \exp(-E/T)$, where $Z = \sum_C P(C)$. T can be positive or negative; "increasing T" is defined as in the previous section. The average energy $\langle E \rangle = \sum_C E(C)P(C)$ is an increasing function of both T and vortex length $L = Nh$.

Define

$$\mu_{N,T} = \frac{\log\langle r_N \rangle}{\log N},$$

where r_N is the end-to-end length of the vortex measured by a straight ruler, or alternatively, the diameter of the vortex as it is usually defined. As $N \to \infty$, h fixed for Nh fixed, $\mu_{N,T}$ tends to a limit μ_T; $1/\mu_T$ is the fractal dimension of the resulting limiting object [C18],[C21].

For fixed, finite N, $\frac{\partial \mu_{N,T}}{\partial T} < 0$; i.e., as T decreases, the vortex becomes an increasingly folded object. In the limit $N \to \infty$, $\mu_T = 1$ for $T < 0$, $\mu_T = 1/3$ for $T > 0$, $\mu_T \cong .59$ for $|T| = \infty$. Note that $|T| = \infty$ is the maximum entropy state.

Suppose now that the "vortex" is imbedded in an Euler flow. Its length will increase, by stretching and by fractalization; $\frac{dN}{dt} > 0$. The average energy is an increasing function of both T and of the vortex length L. If energy is conserved, it follows that $\frac{dT}{dt} < 0$ and the temperature decreases. Also, $\frac{d\mu_N}{dt} < 0$ and the vortices fold, as described at the end of section 5. If the vortex is initially smooth, $T(t = 0) < 0$, and the temperature decreases to $|T| = \infty$. The point $|T| = \infty$ is an attracting fixed point for Euler dynamics; that is where the vortices will end up and generate a Kolmogorov spectrum [C19]. $|T| = \infty$ is an uncrossable barrier for Euler dynamics. Asymptotic vortex structures are poised at the boundary between $T < 0$ and $T > 0$.

Note that as long as N is finite, strong, organized, coherent structures contribute less to the energy dissipation than weaker, incoherent vortices. Indeed, contrast two vortex filaments with the same finite N but different circulations Γ_1, Γ_2, say $\Gamma_1 > \Gamma_2$. The energy integral being proportional to Γ^2, the Gibbs weights attached to the two filaments are $Z^{-1} \exp(-\beta \Gamma_1^2 E)$, $Z^{-1} \exp(-\beta \Gamma_2^2 E)$, where E is the energy that results from $\Gamma = 1$. These weights are the same as those one would obtain with $\Gamma = 1$ and $T_1 = T/\Gamma_1^2$ in the first case, $T_2 = T/\Gamma_2^2$ in the second. If one thinks of $D = 1/\mu_{N,T}$ as an approximate fractal dimension, the vortex with larger Γ has a smaller $|T|$, and if $T < 0$ (which is the physically relevant case), then the vortex with larger Γ has a smaller dimension and appears smoother. Strong vortices are less folded. The more folded vortex has a broader spectrum and thus contributes more to dissipation relative to its energy.

In a numerical calculation, N remains finite, and the $|T| = \infty$ barrier can be crossed. If it is, excess folding and stretching may follow, as is indeed observed. One can reduce

27

this excess by a systematic removal of folds ("hairpins") which can be justified as a renormalization. Hairpin removal thus becomes a very useful tool in vortex methods.

There may however be simpler ways to arrest the crossing of the $|T| = \infty$ barrier. A key observation in this respect is Qi's observation [Q1] that the crossing is most likely to happen where the vortex torsion is zero; such points are readily identifiable before disaster strikes.

8. Remarks on turbulence and on superfluid vortices.

In the previous section we developed a theory of thermal equilibria of vortex filaments and used it to explain the folding instability of computational vortex filaments. The theory can also be applied directly to physical vortices.

In a classical (i.e., non quantum) fluid in turbulent motion vortex filaments typically form a dense suspension; their cross-sections vary rapidly and play a role in the dynamics. The equilibrium theory of filaments is a plausible cartoon of the equilibrium states of vortex filaments in this context, and reveals important features of the motion; it must however be interpreted with some care [C21].

A major conceptual leap that must be made in order to apply the model to turbulence concerns the idea that the inertial range of turbulence can be described by an equilibrium model. In the usual presentation of the Kolmogorov theory, inertial scales do little besides transfer energy from large to small scales, in an irreversible waterfall-like cascade that cannot be assimilated to a thermal equilibrium. However, there is overwhelming experimental [M8] and numerical [C21] evidence that energy goes both up and down the ladder of scales; in other problems, even in Burgers' equation, equilibrium and a power law spec-

trum appear together. An equilibrium with a wide spectrum may enhance dissipation, but not necessarily be dominated by it. This argument is laid out in detail in [C21]. In superfluid (quantum) turbulence these arguments are easier to visualize. In a superfluid, vortices exist as physical entities; their cores are well defined. The dissipation mechanisms (e.g., the Hall-Vinen friction [H3]) do not concentrate at the smallest scales and the simple cascade ideas are not as attractive. Indeed, "fractal" vortex equilibria similar to the ones described above do occur, for example, near the T_λ transition to superfluidity [S4],[W3] or in the related problem of "vortex glasses" in "high temperature" superconductors [H6].

However, some paradoxes appear as soon as one considers turbulence in superfluids more closely. In many important respects, quantum and classical turbulence are very different. Quantum vortices generally look smoother than classical vortices. The rate at which vortex length per unit volume L is generated appears to be proportional to $L^{3/2}w$, where w is a quantum "counterflow" velocity that vanishes in a non-superfluid. By contrast, the rate of change of L in classical turbulence is proportional to L [C21]. Thus vortex stretching appears to be much more important in classical than in quantum turbulence.

A qualitative explanation of these differences is contained in the theory of the last section. The rate of change of L was connected with the rate of change of the temperature T. A classical fluid has a self-adjusting temperature T such that $|T| \rightarrow \infty$, and there are no bounds on L. In a quantum fluid (and maybe also in compressible turbulence) wave/vortex interactions control T and then L may be bounded. Deeper explanations remain to be explored; the relations of quantum to fluid vortex motion are discussed in

[C19],[C21]. Vortex methods appear as the natural tools for analyzing these relations and the structure of turbulence in general.

This may be the place to dwell on a numerical mystery. If vortex stretching and folding are inhibited in quantum turbulence, vortex motion in quantum and classical fluids should be very different. In a partial recognition of this fact, superfluid physicists often replace the Biot-Savart law (9) by a different velocity fluid that depends only on a local curvature of the vortex filament. The equations obtained from this approximation, the "local induction approximation" (LIA) have a very different character from the Euler equations, and in particular they preserve vortex length [B12],[C10]. It is however persistently claimed in the superfluidity literature that the LIA and the Biot-Savart law can be used interchangeably.

In one case, examined by Buttke [B12], it turns out that the resemblance between the LIA and the Euler results claimed in earlier work is an artifact of the numerics; a sufficient refinement of the mesh in the LIA destroys this resemblance. There are however more subtle problems. For example, according to recent work [S1], waves propagate on vortex filaments with only a "confined chaos" and no breakdown of the vortex. A crude enough solution of the Euler equations in this case reproduces the results of the LIA to a good approximation. A more resolved calculation is at sharp variance with the LIA, but an even more refined calculation produces again results that have a qualitative (but not quantitative) similarity to the results obtained by the LIA [Q1]. A deeper understanding of this situation is not yet available.

9. Acknowledgment

References

The literature on vortex methods has become very large; references [C21],[G6],[M4] and [P3] contain extensive bibliographies. I have listed below only those references that are used in the text or that directly extend it. I apologize to all the authors whose work is omitted and assure them that no value judgement is implied.

[A1] A. Almgren, T. Buttke and P. Colella, A fast vortex method in three dimensions, J. Comp. Phys., 1993, in press.

[A2] A. Anderson, A method of local corrections for computing the velocity field due to a distribution of vortex blobs, J. Comput. Phys., 61, 111–123 (1985).

[A3] C. Anderson, An implementation of the fast multipole method without multipoles, CAM report 90-14, UCLA Math. Dept., 1990.

[A4] C. Anderson and C. Greengard, On vortex methods, SIAM J. Sc. Stat. Comp., 22, 413–440 (1985).

[A5] C. Anderson and C. Greengard, The vortex ring merger at infinite Reynolds number, Comm. Pure Appl. Math., 42, 1123–1139 (1989).

[A6] C. Anderson and C. Greengard, Vortex methods, Lecture notes in mathematics, Springer, vol. 1360, 1988.

[A7] A. Appel, An efficient program for many-body simulations, SIAM J. Sc. Stat. Comp., 6, 85–103 (1985).

[B1] J. Barnes and P. Hut, A hierarchical O(NlogN) force calculation algorithm, Nature, 324, 446–449 (1986).

[B2] J.T. Beale, A convergent 3D vortex method with grid-free stretching, Math.

Comp., 46, 401–424 (1986).

[B3] J.T. Beale, T. Kato and A. Majda, Remarks on the breakdown of smooth solutions for the 3D Euler equations, Comm. Math. Phys., 94, 61–66, (1984).

[B4] J.T. Beale and A. Majda, Vortex methods I: Convergence in three dimensions, Math. Comp.,39,1–27 (1982).

[B5] J.T. Beale and A. Majda, Vortex methods II: Higher order accuracy in two and three space dimensions, Math. Comp., 32, 29–52 (1982).

[B6] J.T. Beale and A. Majda, High order accurate vortex methods with explicit velocity kernels, J. Comp. Phys.., 58, 188–208 (1985).

[B7] G. Benfatto and M. Pulvirenti, A diffusion process associated with the Prandtl equation, J. Funct. Anal., 52, 330–343 (1983).

[B8] G. Benfatto and M. Pulvirenti, The convergence of the Chorin-Marsden product formula in the half-plane, Comm. Math. Phys., 106, 427–258 (1986).

[B9] G. Benfatto, P. Picco and M. Pulvirenti, On the invariant measures for the two-dimensional Euler flow, J. Stat. Phys., 46, 729–742 (1987).

[B10] T. Buehler, Vortex approximation of boundary layers, Ph.D. thesis, Math. Dept., Berkeley, 1993.

[B11] T. Burkhardt and J.M.J. van Leeuwen (eds.), Real-space renormalization, Springer, Berlin, 1982.

[B12] T. Buttke, Numerical study of superfluid turbulence in the self-induction approximation, J. Comp. Phys., 76, 301–326 (1988).

[B13] T. Buttke, A fast adaptive vortex method for patches of constant vorticity in two

dimensions, J. Comp. Phys., 89, 161–186 (1990).

[B14] T. Buttke, Hamiltonian structure for 3D incompressible flow, manuscript, 1991.

[B15] T. Buttke, Lagrangian numerical methods which preserve the Hamiltonian structure of incompressible fluid flow, Comm. Pure Appl. Math., 1993, in press.

[B16] T. Buttke and A. Chorin, Turbulence calculations in magnetization variables, to appear in Proc. 1992 Israel/US symposium on scientific computing.

[C1] R. Caflisch, Mathematical analysis of vortex dynamics, SIAM, Philadelphia, 1988.

[C2] E. Caglioti, P.L. Lions, C. Marchioro and M. Pulvirenti, A special class of stationary flows for two-dimensional Euler equations: A statistical mechanics description, Comm. Math. Phys., 1993, in press.

[C3] C.C.Chang, Random vortex methods for the Navier-Stokes equations, J. Comp. Phys., 76, 281–300 (1988).

[C4] A. Cheer, Unsteady separated wake behind an impulsively started cylinder, J. Fluid Mech., 201, 485–505 (1989).

[C5] A.J. Chorin, Vortex methods for rapid flow, Proc. 2d Int. Cong. Num. Meth. Fluid Mech., Springer, 1972.

[C6] A.J. Chorin, Numerical study of slightly viscous flow, J. Fluid Mech., 57, 785–796 (1973).

[C7] A.J. Chorin, Lectures on turbulence theory, Publish/Perish, Berkeley, 1975.

[C8] A.J. Chorin, Vortex models and boundary layer instability, SIAM J. Sc. Stat. Comp., 1, 1–21 (1980).

[C9] A.J. Chorin, Estimates of intermittency, spectra and blow-up in fully developed

turbulence, Comm. Pure Appl. Math., 34, 853–866 (1981).

[C10] A.J. Chorin, The evolution of a turbulent vortex, Comm. Math. Phys., 83, 517–535 (1982).

[C11] A.J. Chorin, Turbulence and vortex stretching on a lattice, Comm. Pure Appl. Math., 39 (special issue), S47–S65 (1986).

[C12] A.J. Chorin, Scaling laws in the lattice vortex model of turbulence, Comm. Math. Phys., 114, 167–176 (1988).

[C13] A.J. Chorin, Spectrum, dimension and polymer analogies in fluid turbulence, Phys. Rev. Lett., 60, 1947–1949 (1988b).

[C14] A.J. Chorin, Computational fluid mechanics, selected papers, Academic, 1989.

[C15] A.J. Chorin, Hairpin removal in vortex interactions, J. Comp. Phys., 91, 1–21 (1990b).

[C16] A.J. Chorin, Vortices, turbulence and statistical mechanics, in "vortex methods and vortex motions", K. Gustafson and J. Sethian (eds.), SIAM, 1991.

[C17] A.J. Chorin, Statistical mechanics and vortex motion, AMS lectures in applied mathematics, 28, 85–101 (1991b).

[C18] A.J. Chorin, Equilibrium statistics of a vortex filament with applications, Comm. Math. Phys., 141, 619–631 (1991d).

[C19] A.J. Chorin, A vortex model with turbulent and superfluid percolation, J. Stat. Phys., 69, 67–78 (1992).

[C20] A.J. Chorin, Hairpin removal in vortex interactions II, J. Comput. Phys., 1993, in press.

[C21] A.J. Chorin, Vorticity and Turbulence, Springer, 1993.

[C22] A.J. Chorin, A model of turbulent phase transitions in 2.5 dimensions, manuscript, 1993.

[C23] A.J. Chorin and J. Akao, Vortex equilibria in turbulence theory and quantum analogues, Physica D, 52, 403–414 (1991).

[C24] A.J. Chorin and P. Bernard, discretization of a vortex sheet with an example of roll-up, J. Comp. Phys., 13, 423–429 (1973).

[C25] A.J. Chorin and J. Marsden, A mathematical introduction to fluid mechanics, Springer, 1979, 1990.

[C26] A.J. Chorin, T. Hughes, M. McCracken and J. Marsden, Product formulas and numerical algorithms, Comm. Pure Appl. Math., 31, 205–252 (1978).

[C27] R. Cortez, The geometry of impulse flow, Manuscript, Math. Dept, UC Berkeley, 1993.

[C28] G.H. Cottet, Methodes particulaires pour l'equation d'Euler dans le plan, These de 3ieme cycle, Univ. P. and M. Curie, Paris, 1982.

[C29] G.H. Cottet, A new approach to the analysis of vortex methods in two and three space dimensions, Ann. Inst. H. Poincare, Anal. Non Lin., 5, 227–285 (1988).

[C30] G.H. Cottet, Large time behavior for deterministic particle approximations to the Navier-Stokes equations, Math. Comp., 56, 45–60 (1991).

[C31] G.H. Cottet and S. Mas-Gallic, A particle method to solve the Navier-Stokes system, Numer. Math., 57, 805–827 (1990).

[D1] R.J. Donnelly, Quantized vortices in Helium II, Cambridge, 1991.

[D2] D. Dritschel, The repeated filamentation of two-dimensional vorticity interfaces, J. Fluid Mech., 194, 511–547 (1988).

[D3] H. Dym and H. McKean, Fourier series and integrals, Academic, 1972.

[E1] G.L. Eyink and H. Spohn, Negative temperature states and equivalence of ensembles for the vortex model of a two-dimensional ideal fluid, J. Stat. Phys., 70, 833–886 (1993).

[E2] R. Esposito and M. Pulvirenti, Three dimensional stochastic vortex flows, 1987, preprint.

[F1] D. Fishelov, Vortex methods for slightly viscous three dimensional flows, SIAM J. Sci. Stat. Comp., 11, 399–424 (1990).

[F2] D. Fishelov, A new vortex scheme for viscous flow, J. Comput. Phys., 86, 211–224 (1990).

[G1] A.F. Ghoniem and G. Heidarinejad, Numerical study of scalar mixing and product formation in a shear layer, Combust. Sci. Tech., 72, 79–99 (1990).

[G2] J. Goodman, The convergence of random vortex methods, Comm. Pure Appl. Math., 40, 189–220 (1987).

[G3] C. Greengard, the core spreading vortex method approximates the wrong equation, J. Comput. Phys., 61, 345–347 (1985).

[G4] C. Greengard, Convergence of the vortex filament method, Math. Comp., 47, 387–398 (1986).

[G5] L. Greengard and V. Rokhlin, A fast algorithm for particle simulations, J. Comput. Phys., 73, 325–348 (1988).

[G6] C. Greengard and E. Thomann, Singular vortex systems and weak solutions of the Euler equations, Phys. Fluids 31, 2810–2812 (1988).

[G7] K. Gustafson and J. Sethian, Vortex methods and vortex flows, SIAM, 1991.

[H1] O.H. Hald, Convergence of vortex methods II, SIAM J. Sc. Stat. Comp., 16, 726–755 (1979).

[H2] O.H. Hald, Convergence of vortex methods for Euler's equations III, SIAM J. Num. Anal., 24, 538–582 (1987).

[H3] H. Hall and W. Vinen, The rotation of liquid Helium II: The theory of mutual friction, Proc. Roy. Soc. London, A 238, 215–233 (1956).

[H4] T.Y. Hou and J. Lowengrub, Convergence of a point vortex method for the 3D Euler equations, Comm. Pure Appl. Math., 43, 965–981 (1990).

[H5] T.Y. Hou and B. Wetton, Convergence of a finite difference scheme for the Navier-Stokes equations using vorticity boundary conditions, SINUM 29, 615–639 (1992).

[H6] D. Huse, M. Fisher and D. Fisher, Are superconductors really superconducting? Nature, 358, 553–559 (1992).

[J1] G. Joyce and D. Montgomery, Negative temperature states for the two-dimensional guiding center plasma, J. Plasma Physics, 10, 107–121 (1973).

[K1] J. Katzenelson, Computational structure of the N-body problem, SIAM J. Sc. Stat. Comp., 10, 787–815 (1989).

[K2] R. Kerr and F. Hussain, Simulation of vortex reconnection, Physica D 37, 474–484 (1989).

[K3] M. Kiessling, Statistical mechanics of classical particles with logarithmic interac-

tions, Comm. Pure Appl. Math., 1993, in press.

[K4] M. Kiya and H. Ishii, Vortex interaction and Kolmogorov spectrum, Fluid Dynamics Res., 8, 73–83 (1991).

[K5] O. Knio and A. Ghoniem, Three dimensional vortex methods, J. Comp. Phys., 86, 75–106 (1990).

[K6] O.M. Knio, and A.F. Ghoniem, Three-dimensional vortex simulation of the rollup and entrainment in a periodic shear layer, J. Comput. Phys., 97, 172–223 (1991).

[K7] O.M. Knio and A.F. Ghoniem, The three-dimensional structure of periodic vorticity layers under non-symmetric conditions, J. Fluid Mechanics, 243, 353–392 (1992).

[K8] J. Kosterlitz, The critical properties of the two-dimensional XY model, J. Phys. C: Solid State Phys., 7, 1046–1060 (1974).

[K9] J. Kosterlitz and D.J. Thouless, Order, metastability and phase transitions in two-dimensional systems, J. Phys. C: Solid State Phys., 6, 1181–1203 (1973).

[K10] P. Koumoutsakos, Direct numerical simulation of unsteady separated flow using vortex methods, Ph.D. thesis, Caltech, 1993.

[K11] R. Krasny, Desingularization of periodic vortex sheet roll-up, J. Comput. Phys., 65, 292–289 (1986).

[K12] R. Krasny, A study of singularity formation in a vortex sheet by the point vortex approximation, J. Fluid Mech., 167, 65–93 (1986).

[K13] R. Krasny, Computing vortex sheet motion, Proc. of the Int. Congress of Math., Kyoto, 1990.

[K14] A. Krishnan and A.F. Ghoniem, Simulation of rollup and mixing in Rayleigh-Taylor flow using the transport-element method, J. Comp. Phys., 99, 1–27 (1992).

[L1] H. Lamb, Hydrodynamics, Dover, NY, 1932.

[L2] A. Leonard, Numerical simulation of interacting three-dimensional vortex filaments, Proc. 4th Int. Conf. Num. Meth. Fluids, Springer, 1975.

[L3] A. Leonard, Computing three dimensional vortex flows with vortex filaments, Ann. Rev. Fluid Mech., 17, 523–559 (1985).

[L4] D.G. Long, Convergence of the random vortex method in two dimensions, J. Am. Math. Soc., 1, 779–804 (1988).

[L5] D.G. Long, Convergence of random vortex methods in three dimensions, In press, Math. Comp., 1993.

[M1] A. Majda, Vorticity and the mathematical theory of incompressible fluid flow, Comm. Pure Appl. Math., 39, S187–S179 (1986).

[M2] A. Majda, Vorticity, turbulence and acoustics in fluid flow, SIAM Review, 33, 349–388 (1991).

[M3] A. Majda, The interaction of nonlinear analysis and modern applied mathematics, Proc. Int. Cong. Math., Kyoto, Japan, 1991.

[M4] C. Marchioro and M. Pulvirenti, Vortex methods in two-dimensional fluid mechanics, Springer, NY, 1984.

[M5] J. Marsden and A. Weinstein, Coadjoint orbits, vortices and Clebsch variables for incompressible fluids, Physica 7, 305–323 (1983).

[M6] L.-F. Martins and A.F. Ghoniem, "Vortex simulation of the flow field in a planar

piston-chamber arrangement with an intake, Int. J. for Num. Meth. in Fluids., 12, 237–260 (1991).

[M7] J. Meng and J. Thompson, Numerical studies of of some nonlinear hydrodynamic problems by discrete vortex element methods, J. Fluid Mech., 84, 433–453 (1978).

[M8] C. Meneveau, Dual spectra and mixed energy cascade of turbulence in the wavelet representation, Phys. Rev. Lett., 66, 1450–1453 (1991).

[M9] J. Miller, Statistical mechanics of Euler equations in two dimensions, Phys. Rev. Lett., 65, 2137–2140 (1990).

[M10] P. Moin, A. Leonard and J. Kim, Evolution of a curved vortex filament into a vortex ring, Phys. Fluids, 29, 955–963 (1986).

[M11] D. Montgomery and G. Joyce, Statistical mechanics of negative temperature states, Phys. Fluids, 17, 1139–1145 (1974).

[M12] D. Montgomery, W. Matthaeus, W. Stribling, D. Martinez and S. Oughton, Relaxation in two dimensions and the "Sinh-Poisson" equation, Phys. Fluids, A 4, 3–6 (1992).

[N1] H. Najm and A.F. Ghoniem, Vortex simulation of the convective instability in a dump combustor, AIAA Journal, 29, 911–919 (1991).

[N2] S. Nemirovski, J. Pakleza and W. Poppe, Stochastic behavior of vortex filaments, LIMSI/CNRS report 91-14, Orsay, 1991.

[N3] M. Nitsche, Axisymmetric vortex sheet roll-up, Ph.D. thesis, Math. Dept., Michigan, 1992.

[N4] H. Nordmark, Higher order vortex methods with rezoning, J. Comput. Phys., 97,

366–397 (1991).

[O1] V.I. Oseledets, On a new way of writing the Navier-Stokes equations: The Hamiltonian formalism, Comm. Moscow Math. Soc. 1988, translated in Russ. Math. Surveys, 44, 210–211 (1989).

[P1] M. Perlman, On the accuracy of vortex methods,J. Comp. Phys., 59, 200–223 (1985).

[P2] E.G. Puckett, A study of the vortex sheet method and its rate of convergence, SIAM J. Sc. Stat. Comp., 10, 298–327 (1989).

[P3] E.G. Puckett, A review of vortex methods, in "Incompressible computational fluid mechanics", R. Nicolaides and M. Ginzburger (eds.), Cambridge, 1992.

[Q1] A. Qi, Three dimensional vortex methods for the analysis of propagation on vortex filaments, Ph.D. thesis, Math. Dept., UC Berkeley, 1991.

[R1] P. Raviart, An analysis of particle methods, Num. Meth. Fluid Mech., F. Brezzi (ed.), Springer, 1985.

[R2] M. Reider, Development of higher order numerical methods for two-dimensional incompressible flow with applications to flow around circular cylinders and airfoils, Ph.D. thesis, Math. Dept., UCLA, 1992.

[R3] R. Robert, A maximum entropy principle for two-dimensional perfect fluid dynamics, J. Stat. Phys., 65, 531–554 (1991).

[R4] P.H. Roberts, A Hamiltonian theory for weakly interacting vortices, Mathematica, 19, 169–179 (1972).

[R5] S. Roberts, Accuracy of the random vortex method for a problem with non-smooth

initial data, J. Comput. Phys., 58, 29–43 (1985).

[R6] S. Roberts, Convergence of random walk methods, Ph.D. thesis, Berkeley, 1986.

[R7] L. Rosenhead, The formation of vortices from a surface of discontinuity, Proc. Roy. Soc. London, A 134, 170–192 (1931).

[R8] A. Rouhi, Poisson brackets for point dipole dynamics in three dimensions, manuscript, UC San Diego, 1990.

[R9] G. Russo and J. Strain, Fast triangulated vortex methods for the 2D Euler equations, J. Comput. Phys., 1993, in press.

[S1] D. Samuels, and R. Donnelly, Sideband instability and recurrence of Kelvin waves on vortex cores, Phys. Rev. Lett., 64, 1385–1388 (1990).

[S2] J. Sethian, J.P. Brunet, A. Greenberg and J. Mesirov, Two dimensional viscous incompressible flow in complex geometry on a massively parallel processor, J. Comput. Phys., 101, 185–206 (1992).

[S3] J. Sethian and A. Ghoniem, A validation study of vortex methods, J. Comp. Phys., 74, 283–317 (1988).

[S4] S.R. Shenoy, Vortex loop scaling in the three-dimensional XY ferromagnet, Phys. Rev. B, 40, 5056–5068 (1989).

[S5] D. Summers, A random vortex simulation of Falkner-Skan boundary layer flow, J. Comput. Phys., 85, 86–103 (1989).

[S6] D. Summers, An algorithm for vortex loop generation, LBL report LBL-31367, Berkeley, CA, 1991.

[T1] G. Tryggvason, Numerical simulations of the Rayleigh-Taylor instability, J. Com-

put. Phys., 75, 252–288 (1988).

[V1] L. Van Dommelen and E. Rundensteiner, Fast adaptive summation of point forces in two-dimensional Poisson equations, J. Comput. Phys., 83, 126–147 (1989).

[W1] H.Y. Wang, A high order vortex method for patches of constant vorticity, Report PAM-534, Math. Dept, Berkeley, 1991.

[W2] S. Widnall, The structure and dynamics of vortex filaments, Ann. Rev. Fluid Mech., 8, 141–165 (1976).

[W3] G. Williams, Vortex ring model of the superfluid lambda transition, Phys. Rev. Lett., 59, 1926–1929 (1987).

[W4] G. Williams, Vortex rings and finite wave-number superfluidity near the 4He lambda transition, Phys. Rev. Lett., 68, 2054–2057 (1992).

[W5] G. Winckelmans and A. Leonard, Contributions to vortex particle methods for the computation of three-dimensional incompressible unsteady flow, J. Comput. Phys., 1993, in press.

[W6] J.C. Wu and J.F. Thompson, Numerical solutions of time-dependent incompressible Navier-Stokes equations using integro-differential equations, Computers and Fluids, 1, 197–215 (1973).

LAWRENCE BERKELEY LABORATORY
UNIVERSITY OF CALIFORNIA
TECHNICAL INFORMATION DEPARTMENT
BERKELEY, CALIFORNIA 94720